

Research Article

Broadband Beam-space DOA Estimation: Frequency-Domain and Time-Domain Processing Approaches

Shefeng Yan

Institute of Acoustics, Chinese Academy of Sciences, 100080 Beijing, China

Received 1 November 2005; Revised 11 April 2006; Accepted 12 May 2006

Recommended by Peter Handel

Frequency-domain and time-domain processing approaches to direction-of-arrival (DOA) estimation for multiple broadband far field signals using beam-space preprocessing structures are proposed. The technique is based on constant mainlobe response beamforming. A set of frequency-domain and time-domain beamformers with constant (frequency independent) mainlobe response and controlled sidelobes is designed to cover the spatial sector of interest using optimal array pattern synthesis technique and optimal FIR filters design technique. These techniques lead the resulting beam-patterns higher mainlobe approximation accuracy and yet lower sidelobes. For the scenario of strong out-of-sector interfering sources, our approaches can form nulls or notches in the direction of them and yet guarantee that the mainlobe response of the beamformers is constant over the design band. Numerical results show that the proposed time-domain processing DOA estimator has comparable performance with the proposed frequency-domain processing method, and that both of them are able to resolve correlated source signals and provide better resolution at lower signal-to-noise ratio (SNR) and lower root-mean-square error (RMSE) of the DOA estimate compared with the existing method. Our beam-space DOA estimators maintain good DOA estimation and spatial resolution capability in the scenario of strong out-of-sector interfering sources.

Copyright © 2007 Hindawi Publishing Corporation. All rights reserved.

1. INTRODUCTION

Broadband direction-of-arrival (DOA) estimation has found numerous applications to radar, sonar, wireless communications, and other areas. Incoherent signal-subspace methods such as [1, 2] perform narrowband DOA estimation for each frequency bin and then statistically combine the resulting estimates to form a broadband DOA estimate. However, coherent signal sources cannot be handled by this approach. The coherent signal subspace (CSS) method was proposed by Wang and Kaveh [3] as an alternative method to deal with coherent signal sources. It decomposes the broadband data into several narrowband frequency bins and finds focusing matrices that transform the covariance matrices of each bin into the one corresponding to the reference frequency bin. Conventional narrowband DOA estimation methods such as MUSIC [4] may then be directly applied to find the directions of arrival. CSS methods have been found to exhibit better resolution at low signal-to-noise ratio (SNR) and lower estimate variance than incoherent methods. However, the design of focusing matrices in the CSS method requires preliminary DOA estimates in the neighborhood of the true directions of arrival.

Other broadband DOA estimation methods based on the beam-space preprocessing are proposed in [5, 6]. The beam-space preprocessing is performed by using frequency-invariant beamformers (FIBs) that transform the element-space into the beam-space. The beamforming matrices perform the same operation as focusing matrices in the CSS method, but without preliminary DOA estimates. In [5], Lee constructs a beamforming matrix for each frequency bin such that the resulting beam-patterns are essentially identical for all frequencies by solving a least squares optimization problem. However, the least squares fit is employed not only in the mainlobe but also in the sidelobe regions, which leads to suboptimal designs since the sidelobes only need to be guaranteed to remain below the prescribed threshold value. In [6], Ward et al. present a DOA estimator that performs broadband focusing using time-domain processing, in which a set of appropriately designed beam-shaping filters [7] ensure that the similar array pattern is produced for all frequencies within the design band. The estimator need not perform frequency decomposition. However, the FIBs may not be achieved for arrays with arbitrary geometry and nonuniform interelement spacing. Moreover, it is difficult to control the mainlobe width and sidelobe level. Furthermore,

the robustness of the beamformers designed in [5, 6] may decrease since the beamforming weights can be very large. We will refer to the beamspace preprocessing approaches in [5, 6] as frequency-domain frequency-invariant beamspace (FD-FIBS) approach and time-domain frequency-invariant beamspace (TD-FIBS) approach, respectively.

In this paper, new broadband DOA estimation approaches are proposed by designing a set of frequency-domain and time-domain beamformers with constant mainlobe response over the design band to cover the spatial sector of interest. We will refer to the beamformer with constant mainlobe response as *constant mainlobe response beamformer* (CMRB). The frequency-domain weight vector of CMRB is designed using optimal array pattern synthesis techniques to ensure that the resulting beampattern is constant within the mainlobe over the design band while guarantee the sidelobes to be below the prescribed values. For our array pattern synthesis problems, the least squares fit process is only performed within the mainlobe, which can lead to higher mainlobe approximation accuracy. For our time-domain beamformer, a bank of FIR filters corresponding to the input channels are designed to provide the frequency responses that approximate the frequency-domain array weights for each sensor. Both the array pattern synthesis and the FIR filter design problems are formulated as the second-order cone programming (SOCP), which can be solved efficiently using the well-developed interior-point methods [8, 9]. The SOCP approach has been exploited in robust array interpolation [10] and robust beamforming [11, 12]. The proposed DOA estimators are able to resolve correlated source signals and can be applicable to arrays of arbitrary geometry. For the scenario of strong out-of-sector interfering sources, our estimators can maintain good DOA estimation and spatial resolution capability by forming nulls or notches in the corresponding directions and yet guarantee that the mainlobe response of the broadband beamformer is constant over the design band.

The paper is organized as follows. A brief review of broadband beamspace DOA estimation is presented in Section 2. In Section 3, the frequency-domain and time-domain CMRBs are designed using SOCP approach. In Section 4, the frequency-domain and time-domain processing methods for beamspace DOA estimation are presented. Section 5 presents simulation results confirming the efficiency of the proposed methods, and Section 6 concludes the paper.

2. BACKGROUND

Consider an N -element array with a known arbitrary geometry. Assume that $D < N$ far field broadband sources impinge on the array from directions $\Theta = [\theta_1, \dots, \theta_d, \dots, \theta_D]$. The time series received at the n th element is

$$x_n(t) = \sum_{d=1}^D s_d[t - \xi_n(\theta_d)] + v_n(t), \quad n = 1, \dots, N, \quad (1)$$

where $s_d(t)$ is the d th source signal, $\xi_n(\theta_d)$ is the propagation delay to the n th sensor associated with the d th source, and $v_n(t)$ is the additive white noise. With suitable data segmentation and Fourier transform, the frequency response of the $N \times 1$ complex array data snapshot vector is given by

$$\mathbf{x}(f_j) = \mathbf{A}(\Theta, f_j)\mathbf{s}(f_j) + \mathbf{v}(f_j), \quad (2)$$

where the argument f_j denotes the dependence of the array data on different frequency bins, $\mathbf{s}(f_j) = [s_1(f_j), \dots, s_D(f_j)]^T$ is the $D \times 1$ source signal vector. Here $(\cdot)^T$ denotes the transpose. $\mathbf{v}(f_j)$ is the $N \times 1$ additive noise vector, and $\mathbf{A}(\Theta, f_j) = [\mathbf{a}(\theta_1, f_j), \dots, \mathbf{a}(\theta_D, f_j)]$ is the $N \times D$ source direction matrix with $\mathbf{a}(\theta_d, f_j) = [e^{-i2\pi f_j \xi_1(\theta_d)}, \dots, e^{-i2\pi f_j \xi_N(\theta_d)}]^T$ ($d = 1, \dots, D$) being the array manifold vector. Here $i = \sqrt{-1}$.

In beamspace eigen-based methods, multiple beams are formed over the spatial sector of interest by using a set of K ($D < K < N$) beamforming weight vectors $\mathbf{w}_{jk} = [w_1(f_j, k), \dots, w_n(f_j, k), \dots, w_N(f_j, k)]^T$, $j = 1, \dots, J$, $k = 1, \dots, K$. Here $w_n(f_j, k)$ is the weight of the k th beamformer associated with the n th sensor employed at the frequency bin f_j . Assume that the pointing directions of the K beamformers are $\Phi = [\phi_1, \dots, \phi_k, \dots, \phi_K]$. The received elementspace data snapshot vectors are converted into a reduced dimension beamspace data snapshot vector via the matrix transformation

$$\begin{aligned} \mathbf{y}(f_j) &= \mathbf{W}_j^H \mathbf{x}(f_j) = \mathbf{W}_j^H \mathbf{A}(\Theta, f_j) \mathbf{s}(f_j) + \mathbf{W}_j^H \mathbf{v}(f_j) \\ &= \mathbf{B}(\Theta, f_j) \mathbf{s}(f_j) + \mathbf{v}_B(f_j), \end{aligned} \quad (3)$$

where $\mathbf{B}(\Theta, f_j) = \mathbf{W}_j^H \mathbf{A}(\Theta, f_j)$ and $\mathbf{v}_B(f_j) = \mathbf{W}_j^H \mathbf{v}(f_j)$ are the beamspace DOA matrices and noise vectors, respectively. Here $(\cdot)^H$ denotes the Hermitian transpose. And $\mathbf{W}_j = [\mathbf{w}_{j1}, \mathbf{w}_{j2}, \dots, \mathbf{w}_{jK}]$ is the $N \times K$ beamforming matrices employed at the frequency bin f_j .

Assume that we apply the constant (frequency independent) mainlobe response beamforming technique. Then the response of the beamformer may be made approximately constant within the mainlobe over the design band, that is,

$$\begin{aligned} p_k(\theta, f_j) &= \mathbf{w}_{jk}^H \mathbf{a}(\theta, f_j) \approx p_{\text{CMRB},k}(\theta), \\ j &= 1, \dots, J, \quad k = 1, \dots, K, \quad \theta \in \Theta_M, \end{aligned} \quad (4)$$

where $p_{\text{CMRB},k}(\theta)$ is the constant mainlobe response associated with the k th beamformer, Θ_M is the mainlobe angular region, in contrast to the methods in [5, 6], where the beamformers are designed to ensure that the resulting beampattern is constant over both the mainlobe and the sidelobe regions.

Because the constant response property of the beamformers, the beamspace DOA matrices are approximately constant for all frequencies, that is,

$$\mathbf{B}(\Theta, f_j) \approx \mathbf{B}(\Theta), \quad j = 1, \dots, J. \quad (5)$$

Hence, the broadband source directions are completely characterized by a single beamspace DOA matrix $\mathbf{B}(\Theta)$.

Assuming the source signals and the noise are uncorrelated, the constant mainlobe response beamspace (CMRBS) data covariance matrix is

$$\begin{aligned} \mathbf{R}_y(f_j) &= E\{\mathbf{y}(f_j)\mathbf{y}^H(f_j)\} \\ &= \mathbf{B}(\Theta)E\{\mathbf{s}(f_j)\mathbf{s}^H(f_j)\}\mathbf{B}^H(\Theta) \\ &\quad + \mathbf{W}_j^H E\{\mathbf{v}(f_j)\mathbf{v}^H(f_j)\}\mathbf{W}_j \\ &= \mathbf{B}(\Theta)\mathbf{R}_s(f_j)\mathbf{B}^H(\Theta) + \mathbf{R}_v(f_j), \end{aligned} \quad (6)$$

where $\mathbf{R}_s(f_j) = E\{\mathbf{s}(f_j)\mathbf{s}^H(f_j)\}$ is the $D \times D$ source covariance matrix, and $\mathbf{R}_v(f_j) = \mathbf{W}_j^H E\{\mathbf{v}(f_j)\mathbf{v}^H(f_j)\}\mathbf{W}_j$ is the $K \times K$ CMRBS noise covariance matrix. The broadband CMRBS data covariance matrix can be formed as

$$\begin{aligned} \mathbf{R}_y &= \sum_{j=1}^J \mathbf{R}_y(f_j) \\ &= \sum_{j=1}^J [\mathbf{B}(\Theta)\mathbf{R}_s(f_j)\mathbf{B}^H(\Theta)] + \sum_{j=1}^J \mathbf{R}_v(f_j) \\ &= \mathbf{B}(\Theta) \left[\sum_{j=1}^J \mathbf{R}_s(f_j) \right] \mathbf{B}^H(\Theta) + \mathbf{R}_v, \end{aligned} \quad (7)$$

where $\mathbf{R}_v = \sum_{j=1}^J \mathbf{R}_v(f_j)$ is the broadband beamspace noise covariance matrix.

The broadband CMRBS data covariance matrix (7) is now in a form in which conventional eigen-based DOA estimators may be applied. Denote the eigen-decomposition of matrix pencil $(\mathbf{R}_y, \mathbf{R}_v)$ as (see also [3])

$$\mathbf{R}_y \mathbf{E} = \Lambda \mathbf{R}_v \mathbf{E}, \quad (8)$$

where Λ is the diagonal matrix of sorted eigenvalues, $\mathbf{E} = [\mathbf{E}_s, \mathbf{E}_v]$ contains the corresponding eigenvectors with \mathbf{E}_s and \mathbf{E}_v being the eigenvectors corresponding to the largest D eigenvalues and to the smallest $K-D$ eigenvalues, respectively.

For the MUSIC algorithm [4], the source directions are given by the D peak positions of the following spatial spectrum:

$$P(\theta) = \frac{\mathbf{b}^H(\theta)\mathbf{b}(\theta)}{\mathbf{b}^H(\theta)\mathbf{E}_v\mathbf{E}_v^H\mathbf{b}(\theta)}, \quad (9)$$

where $\mathbf{b}(\theta)$ is the transformed steering vector in beamspace. It is defined as $\mathbf{b}(\theta) = \mathbf{W}^H(f)\mathbf{a}(\theta, f)$ for some $f = f_j$, $j = 1, \dots, J$.

3. DESIGN OF CONSTANT MAINLOBE RESPONSE BEAMFORMER

Concentrate on one of the K beamformers, for example, the k th beamformer, and omit the k symbol temporarily for convenience. The other beamformers can be designed by the same procedure.

3.1. Frequency-domain beamformer

For a reference beampattern, it is preferable to employ beamformers exhibiting high gain within the desired spatial sector and yet uniformly low sidelobes in order to suppress unwanted out-of-sector interfering sources. Let f_0 be the reference frequency, which need not be one of f_j ($j = 1, \dots, J$). Let $\theta_s \in \Theta_S$ ($s = 1, \dots, S$) and $\theta_m \in \Theta_M$ ($m = 1, \dots, M$) be a chosen grid that approximates the sidelobe region Θ_S , and the mainlobe region Θ_M , respectively, using a finite number of angles. The design of reference beampattern, say $p_d(\theta, f_0)$, can be stated as

$$\begin{aligned} \min_{\mathbf{w}_0} \mathbf{w}_0^H \mathbf{R}_n \mathbf{w}_0, \\ \text{subject to } p_d(\phi_0, f_0) = 1, \end{aligned} \quad (10)$$

$$|p_d(\theta_s, f_0)| \leq \delta, \quad \forall \theta_s \in \Theta_S,$$

where \mathbf{w}_0 is the optimal weight vector, that is, design variable, and $p_d(\theta, f_0) = \mathbf{w}_0^H \mathbf{a}(\theta, f_0)$, \mathbf{R}_n is the noise covariance matrix at the reference frequency f_0 which becomes an identity matrix for the special case of spatially white noise, ϕ_0 is the pointing direction of the beamformer, and δ is the prescribed sidelobe value.

The optimal weight vector employed at the frequency bin f_j , say \mathbf{w}_{j0} , can be obtained by solving the following least squares optimization problem:

$$\begin{aligned} \min_{\mathbf{w}_{j0}} \left(\sum_{m=1}^M |p_d(\theta_m, f_0) - p(\theta_m, f_j)|^2 \right), \quad \theta_m \in \Theta_M, \\ \text{subject to } |p(\theta_s, f_j)| \leq \delta_s, \quad \forall \theta_s \in \Theta_S, \\ \|\mathbf{w}_{j0}\| \leq \Delta, \end{aligned} \quad (11)$$

where $p(\theta, f_j) = \mathbf{w}_{j0}^H \mathbf{a}(\theta, f_j)$ is the so-obtained beampattern at the frequency bin f_j , δ_s ($s = 1, \dots, S$) are the desired sidelobe values which can be prescribed to satisfy various requirements. It can even be prescribed to provide nulls or notches to suppress strong out-of-sector interferences. The constraint $\|\mathbf{w}_{j0}\| \leq \Delta$ limits the white-noise gain to improve the beamformer robustness against random errors in array characteristics [13].

The optimization problems (10) and (11) can be formulated as the SOCP problem, which can be efficiently solved using the well-established interior point algorithms, for example, by SeDuMi MATLAB toolbox [8]. A review of the applications of SOCP can be found in [9].

3.2. Time-domain beamformer

Time-domain broadband beamformers can be implemented by placing a tapped delay line or FIR filter at the output of each sensor [14–16]. Each sensor feeds an FIR filter and the filter outputs are summed to produce the beam output time series. In a time-domain CMRB, the sensor filters perform the role of beam shaping and ensure that the beam shape is constant as a function of frequency within the mainlobe.

Assume that the FIR filter associated with the n th sensor is $\mathbf{h}_n = [h_n(1), \dots, h_n(L), \dots, h_n(L)]^T$. Here L is the length of

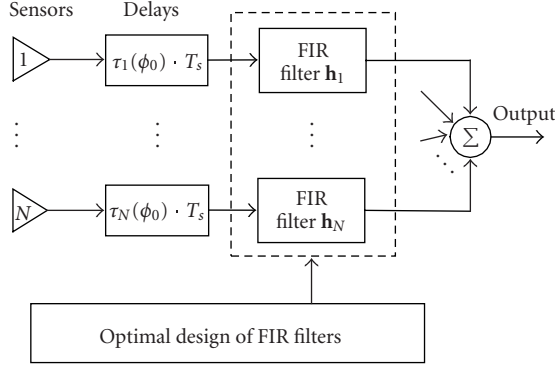


FIGURE 1: FIR broadband beamformer structure.

the filter and \mathbf{h}_n is a real vector. Its corresponding frequency response at frequency f_j is $H_{n,d}(f_j)$, and should equal approximately the array weight $w_n(f_j)$ employed at frequency f_j . The key problem of the time-domain broadband beamformer is how to design the FIR filters.

The inherent group delay (unit in taps) of an FIR filter of length L is nearly $(L - 1)/2$. The group delay of the desired FIR filter is not exactly equal to $(L - 1)/2$ in general, and can be decomposed into an integer part plus a decimal part. We assume that the needed presteering delay (unit in taps) that aligns the desired signal arrived from ϕ_0 (the pointing direction of the beamformer) for channel n is $\zeta_n(\phi_0)$. The array weight can be thus rewritten as [17]

$$w_n(f_j) = e^{-i2\pi f_j \text{int}[\zeta_n(\phi_0) - (L-1)/2]T_s} \cdot w_n(f_j) e^{i2\pi f_j \text{int}[\zeta_n(\phi_0) - (L-1)/2]T_s}, \quad (12)$$

where T_s is the sampling interval and $\text{int}[\cdot]$ denotes round towards nearest integer. The first part of (12) can be implemented by a tapped delay-line delay of $\tau_n(\phi_0) = \text{int}[\zeta_n(\phi_0) - (L - 1)/2]$ taps (when it is minus, a plus integral number can be added for all channels), and the second part by an FIR filter. Thus, the desired frequency response of an FIR filter associated with the n th sensor can be expressed as

$$H_{n,d}(f_j) = w_n(f_j) e^{i2\pi f_j \tau_n(\phi_0) T_s}, \quad j = 1, 2, \dots, J, \quad n = 1, 2, \dots, N, \quad (13)$$

The structure of FIR broadband beamformer with pointing direction ϕ_0 is shown in Figure 1.

The complex frequency response corresponding to the impulse response \mathbf{h}_n is given by

$$H(f) = \sum_{l=1}^L h_n(l) e^{-i(l-1)2\pi f/f_s} = \mathbf{e}^T(f) \mathbf{h}_n, \quad (14)$$

where $\mathbf{e}(f) = [1, e^{-i2\pi f/f_s}, \dots, e^{-i(L-1)2\pi f/f_s}]^T$ and f_s is the sampling frequency.

Let F_p be the stopband, which is discretized using a finite number of frequencies $f_p \in F_p$ ($p = 1, 2, \dots, P$). The design problem of FIR filter associated with the n th sensor is then

stated as

$$\min_{\mathbf{h}_n} \left(\sum_{j=1}^J |H_{n,d}(f_j) - \mathbf{e}^T(f_j) \mathbf{h}_n|^2 \right), \quad (15)$$

subject to $|\mathbf{e}^T(f_p) \mathbf{h}_n| \leq \varepsilon, \quad \forall f_p \in F_p,$

where ε is the prescribed stopband attenuation.

The optimization problems (15) can also be formulated as a second-order cone programming problem. An SOCP-based solving procedure for an FIR filter design can be found in our earlier paper [18].

4. CONSTANT MAINLOBE RESPONSE BEAMSPACE DOA ESTIMATION

4.1. Frequency-domain processing

The frequency-domain processing structure for DOA estimation is shown in Figure 2(a). Assume we apply CMRBs to the received array data in frequency domain. The K -dimensional time series of the K conjunctive beamformer outputs at the frequency bin f_j is given by

$$\mathbf{y}(f_j, q) = \mathbf{W}_j^H \mathbf{x}(f_j, q), \quad (16)$$

where q is the snapshot index. The $K \times K$ beamspace data covariance matrix of the K beamformer outputs at the frequency bin f_j can be estimated from the data vector $\mathbf{y}(f_j, q)$ over a finite series of snapshots $q = 1, 2, \dots, Q$,

$$\hat{\mathbf{R}}_y(f_j) = \frac{1}{Q} \sum_{q=1}^Q [\mathbf{y}(f_j, q) \mathbf{y}^H(f_j, q)], \quad (17)$$

The broadband beamspace data covariance matrix is then constructed by coherently combining the sample covariance matrices

$$\hat{\mathbf{R}}_y = \sum_{j=1}^J \hat{\mathbf{R}}_y(f_j). \quad (18)$$

Assuming the element space noise covariance matrix, that is, $E\{\mathbf{v}(f_j) \mathbf{v}^H(f_j)\}$, is known, then the broadband beamspace noise covariance matrix can be formed as

$$\mathbf{R}_v = \sum_{j=1}^J [\mathbf{W}_j^H E\{\mathbf{v}(f_j) \mathbf{v}^H(f_j)\} \mathbf{W}_j]. \quad (19)$$

In the specific case in which the noise is spatially white and uncorrelated from sensor to sensor, the beamspace noise covariance matrix is

$$\mathbf{R}_v = \frac{\sigma^2}{J} \sum_{j=1}^J [\mathbf{W}^H(f_j) \mathbf{W}(f_j)], \quad (20)$$

where σ^2 is the noise power. If \mathbf{W} is not unitary, then the noise will get colored after multiplication with \mathbf{W} .

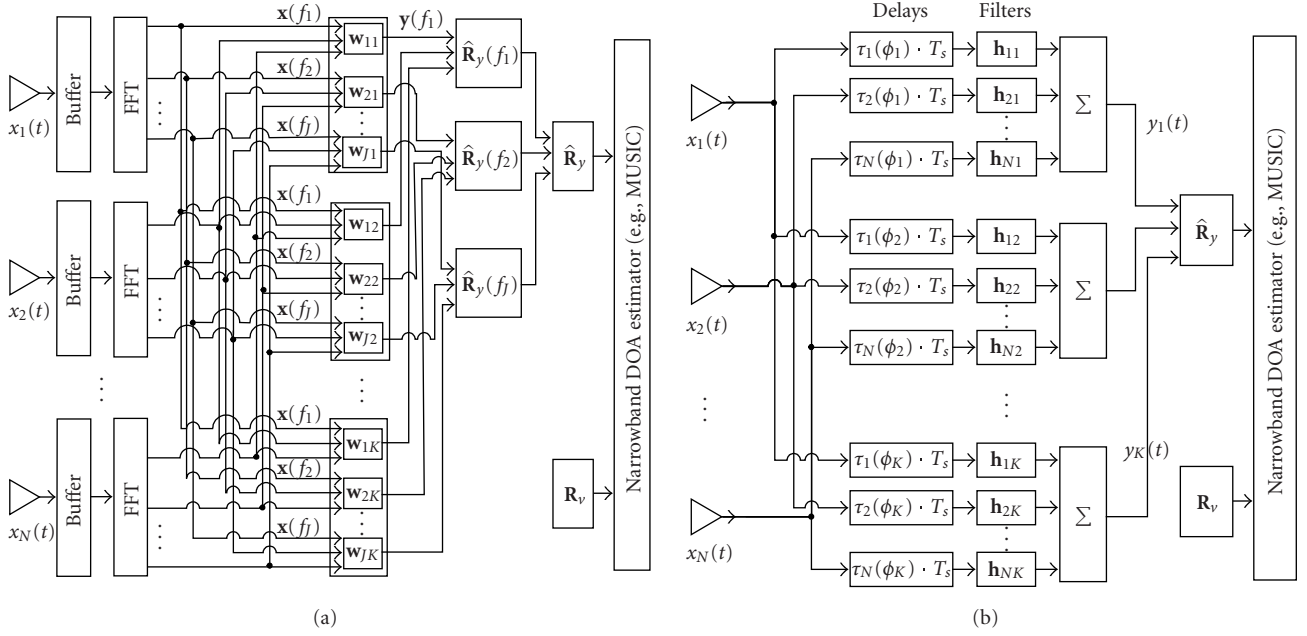


FIGURE 2: Broadband DOA estimation using CMRBs. (a) Frequency-domain processing structure. (b) Time-domain processing structure.

4.2. Time-domain processing

The time-domain processing structure for DOA estimation is shown in Figure 2(b). Let $\mathbf{h}_{nk} = [h_{nk}(1), \dots, h_{nk}(L) \dots, h_{nk}(L)]^T$ be the filter associated with the n th sensor employed at the k th beamformer. The time series of the k th beamformer output is given by

$$y_k(t) = \sum_{n=1}^N \sum_{l=1}^L h_{nk}(l) x_n[t - (l-1) - \tau_n(\phi_k)], \quad (21)$$

where t is the time index.

The K -dimensional time series of the K conjunctive beamformer outputs is given by

$$\mathbf{y}(t) = [\tilde{y}_1^T(t), \dots, \tilde{y}_k^T(t), \dots, \tilde{y}_K^T(t)]^T, \quad (22)$$

where $\tilde{y}_k(t)$ is the discrete-time analytic signal of $y_k(t)$, which can be obtained via a Hilbert transform. Note that since focusing is performed by a set of FIR filters in the time domain, it is unnecessary to perform frequency decomposition in order to form the beamspace data covariance matrix. The broadband beamspace data covariance matrix can be formed from the K -dimensional beamformer outputs over a finite time period $t = 1, 2, \dots, T$.

$$\hat{\mathbf{R}}_y = \frac{1}{T} \sum_{t=1}^T [\mathbf{y}(t) \mathbf{y}^H(t)]. \quad (23)$$

From (13), we see that the virtual beamforming weights employed at frequency f associated with the n th sensor and the k th beamformer is

$$\hat{w}_n(f, k) = H_{nk}(f) e^{-i2\pi f \tau_n(\phi_k) T_s}, \quad (24)$$

where $H_{nk}(f) = \mathbf{e}^T(f) \mathbf{h}_{nk}$ is the resulting frequency response of the FIR filters associated with the n th sensor and the k th beamformer.

The broadband beamspace noise covariance matrix can now be formed as

$$\mathbf{R}_v = \int_{f_L}^{f_U} \widehat{\mathbf{W}}^H(f) E\{\mathbf{v}(f) \mathbf{v}^H(f)\} \widehat{\mathbf{W}}(f) df, \quad (25)$$

where

$$\widehat{\mathbf{W}}(f) = \begin{bmatrix} \hat{w}_1(f, 1) & \cdots & \hat{w}_1(f, K) \\ \vdots & \ddots & \vdots \\ \hat{w}_N(f, 1) & \cdots & \hat{w}_N(f, K) \end{bmatrix} \quad (26)$$

is the virtual $N \times K$ beamforming matrix and $[f_L, f_U]$ is the design band. The integral operation can be represented approximately in a sum form by discretizing the frequency band.

In the specific case in which the noise is spatially white and uncorrelated from sensor to sensor, the broadband beamspace noise covariance matrix is

$$\mathbf{R}_v = \frac{\sigma^2}{f_U - f_L} \int_{f_L}^{f_U} \widehat{\mathbf{W}}^H(f) \widehat{\mathbf{W}}(f) df. \quad (27)$$

4.3. Summary of DOA estimation algorithms

We will refer to the proposed frequency-domain and time-domain constant mainlobe response beamspace processing DOA estimators as the FD-CMRBS approach and the TD-CMRBS approach, respectively.

An outline of the FD-CMRBS broadband DOA estimator is given as follows.

- (1) Design K reference beamformers (10) and then K CM-RBs (11) that cover the spatial region of interest.
- (2) Calculate the broadband beamspace noise covariance matrix \mathbf{R}_v (19) or (20).
- (3) Calculate the K -dimensional beamformer outputs at each frequency bin (16), and estimate the broadband beamspace data covariance matrix $\hat{\mathbf{R}}_y$ (18) from the beamformer outputs over a finite snapshot period.
- (4) Estimate the DOA of the sources from $\hat{\mathbf{R}}_y$ and \mathbf{R}_v using a conventional narrowband DOA estimator such as MUSIC (9).

For the FD-CMRBS DOA estimator, the beamforming matrix can be calculated offline, and the broadband beamspace noise covariance matrix needs only to be calculated once, also offline, if the noise covariance does not change over the observation time.

An outline of the TD-CMRBS broadband DOA estimator is given as follows.

- (1) Design K reference beamformer (10) and then K CM-RBs (11) that cover the spatial region of interest.
- (2) Calculate the desired frequency response of the FIR filters associated with each sensor for each of the K beamformers from frequency-domain weight vectors (13), and then design the filters (15).
- (3) Calculate the virtual beamforming weights (24) from the FIR filters.
- (4) Calculate the broadband beamspace noise covariance matrix \mathbf{R}_v (25) or (27).
- (5) Calculate the K -dimensional time series of the K beamformer outputs (22), and estimate the broadband beamspace data covariance matrix $\hat{\mathbf{R}}_y$ (23) from the beamformer outputs over a finite time period.
- (6) Estimate the DOA of the sources from $\hat{\mathbf{R}}_y$ and \mathbf{R}_v using a conventional narrowband DOA estimator such as MUSIC (9).

For the TD-CMRBS DOA estimator, the FIR filters can be calculated offline, and the broadband beamspace noise covariance matrix can also be calculated once, also off line.

4.4. Computational complexities

The major computational demand of the broadband beamspace DOA estimators comes from the implementation of broadband beamformers.

For the frequency-domain implementation, we assume the FFT length is ℓ , which is assumed to be a power of 2. The computation of the FFT for the data obtained from all the N sensors requires a computational complexity of $N \times \ell \times \log_2 \ell$ complex multiplications. In the weight-and-sum stage, to form K beams, it requires a complexity of $N \times J \times K$ complex multiplication. The overall complexity of frequency-domain broadband beamforming for a block of ℓ data samples is $N \times \ell \times \log_2 \ell + N \times J \times K$ complex multiplication.

If the percentage of the overlap among the input blocks is α , the overall complexity will be $(N \times \ell \times \log_2 \ell + N \times J \times K)/(1 - \alpha)$ complex multiplication. If the sliding window

technique is used, in which the FFT is computed each time a new sample enters the buffer, the complexity of frequency-domain broadband beamforming for the ℓ data samples will be $(N \times \ell \times \log_2 \ell + N \times J \times K) \times \ell$ complex multiplication.

For the time-domain implementation, the beam output time series is produced when each new data sample arrives, in contrast to the FFT beamformer, which requires a block of samples to perform the FFT. Since the tap weights of the FIR filters are real, to form K beams, the overall complexity of time-domain broadband beamforming for the ℓ data samples is $N \times \ell \times L \times K$ real multiplication, in which the computational complexity of a real multiplication is 4 times less than that of a complex multiplication.

Therefore, if the parameters are chosen to be some reasonable values (such as those used in Section 5), the time-domain implementation has a higher computational complexity as compared to the frequency-domain implementation without overlap, while less than that of the frequency-domain implementation with the sliding window technique.

5. SIMULATIONS

5.1. DOA estimation for correlated sources

Consider a linear array of $N = 15$ uniformly spaced elements, with a half-wavelength spacing at the center frequency, also chosen as the reference frequency, $f_0 = 0.3125$ (The normalized sampling frequency was 1). The normalized design band $[f_L, f_U] = [0.25, 0.375]$ is decomposed into $J = 33$ uniformly distributed subbands. $K = 4$ CM-RBs are designed to cover the spatial sector $[0^\circ, 22.5^\circ]$ with respect to the broadside of the array, that is, $\{\phi_k\}_{k=1}^4 = \{0^\circ, 7.5^\circ, 15^\circ, 22.5^\circ\}$. The corresponding beampatterns at all the 33 frequency bins are shown in Figure 3(a). The variation with frequency of the beampattern directed towards 0° is shown in Figure 3(b), from which it is seen that the resulting beampattern within the mainlobe is approximately constant over the frequency band and the sidelobes are strictly guaranteed to be below -30 dB. Just as we desired, the SOCP-based optimal array pattern synthesis approach provides small synthesized errors to CMRBs.

The desired frequency response of the FIR filters associated with each sensor for each beamformer is calculated from the array weights via (13). The desired magnitude and phase responses within the design band associated with the 5th sensor for the first beamformer is shown in Figure 3(c) (with “.”). Assume that the length of each FIR filter is $L = 64$. By solving the optimization problem (15), the magnitude and phase responses of the resulting FIR filter are shown in Figure 3(c). Similar results were obtained for the other FIR filters.

The beampatterns of the time-domain FIR beamformer are calculated at the same 33 frequency bins and shown in Figure 3(d), from which it is seen that the mainlobe response of the resulting beampattern is approximately constant over the entire design band. The time-domain broadband CMRB is implemented with satisfying beampatterns. The sidelobes are just a little higher than that of the frequency-domain

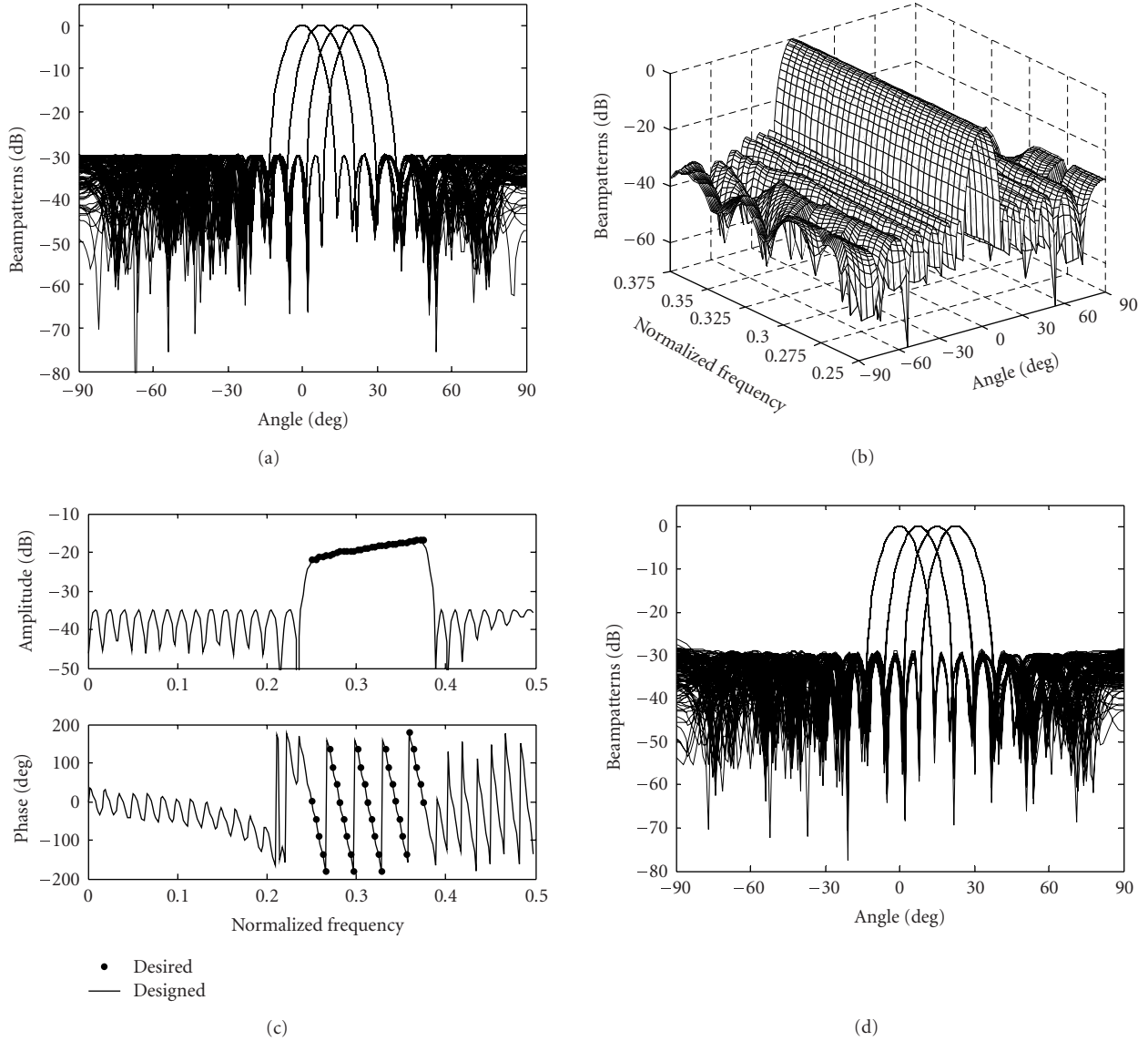


FIGURE 3: Design of the CMRBs. (a) Superposition of the beampatterns of frequency-domain CMRBs in $K = 4$ directions at $J = 33$ frequencies. (b) Variation of beampattern with frequency for the beamformer of 0° . (c) Frequency response of the FIR filter associated with the 5th sensor of the first beamformer. (d) Superposition of the beampatterns of time-domain CMRBs in $K = 4$ directions calculated at $J = 33$ frequencies.

beampatterns since there exist some errors, which are very small and acceptable, between the desired and the designed filters.

A set of simulations was performed to compare the performance of the proposed FD-CMRBS and TD-CMRBS DOA estimators with the FD-FIBS DOA estimator proposed by Lee in [5]. Signals from two correlated sources arrived at $\theta_1 = 8^\circ$ and $\theta_2 = 11^\circ$. The first source signal is assumed to be a bandpass white Gaussian process with flat spectral density over the design band. The second source signal is a delayed version of the first one. The delay at the first sensor (the spatial reference point) is $10T_s$. A spatially white Gaussian bandpass noise with flat spectral density, independent of the received signals, was present at each array

element. The received data was decomposed into $J = 33$ frequency bins using an unwrapped FFT of length $\ell = 256$. For our frequency-domain processing approach, 30 snapshots were used to calculate each DOA estimate. Thus, a total of $256 \times 30 = 7680$ data samples were used for each DOA estimation. The same amount of data samples was used for each DOA estimator. The conventional MUSIC DOA estimator is used on the beamformer outputs for each approach.

Figure 4 shows the spatial spectra of the three broadband beamspace DOA estimators when the SNR is 6 dB. All the approaches are able to resolve the correlated source signals. Our TD-CMRBS DOA estimator has comparable performance with our FD-CMRBS estimator, and, as expected, both of them outperform the FD-FIBS.

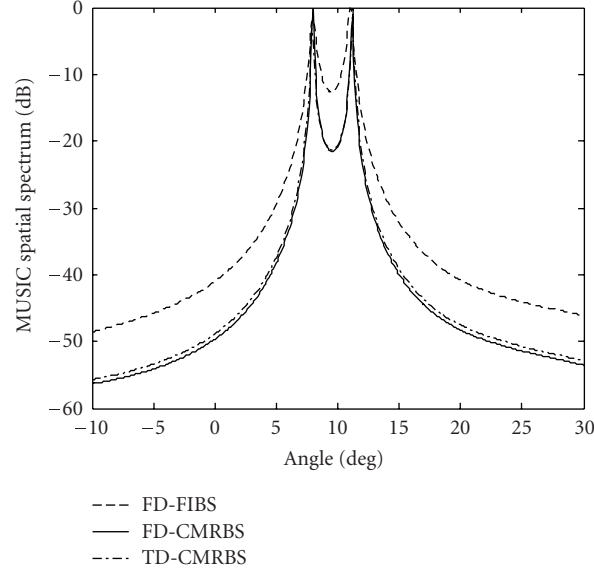


FIGURE 4: DOA estimation result for two correlated sources using FD-FIBS, FD-CMRBS, and TD-CMRBS.

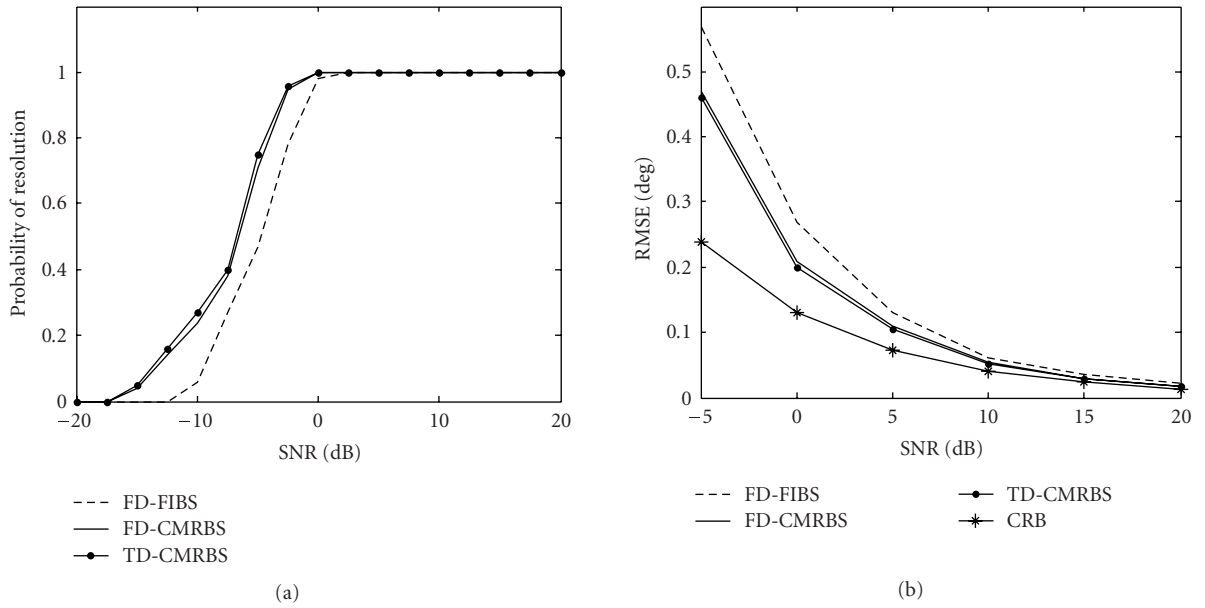


FIGURE 5: Performance comparison of FD-FIBS, FD-CMRBS, and FD-CMRBS for several SNR values. (a) Comparison of the resolution performance. (b) Comparison of the RMSEs.

The probability of resolution versus SNR for the two sources is shown in Figure 5(a). Results are based on 100 independent trials for each SNR, using the same array data for each approach. The signal sources are said to be resolved in a trial if [19]

$$\sum_{d=1}^2 |\hat{\theta}_d - \theta_d| < |\theta_1 - \theta_2|, \quad (28)$$

where $\hat{\theta}_d$ is the DOA estimate of the d th source in the trial.

The resulting sample root-mean-squared error (RMSE) of the DOA estimate of the source at $\theta_1 = 8^\circ$, obtained from 100 independent trials, is shown in Figure 5(b). These results also show that the performance of TD-CMRBS is comparable with that of FD-CMRBS, and that our approaches exhibit better resolution performance than that of FD-FIBS. Also plotted in Figure 5(b) is the square root of Cramer-Rao bound (CRB) of the source at 8° , which is numerically calculated by the procedure given in the appendix of [3]. The RMSEs of our DOA estimators (FD-CMRBS and TD-CMRBS) are seen to be very close to the square root of CRB, which confirm the efficiency of the proposed methods.

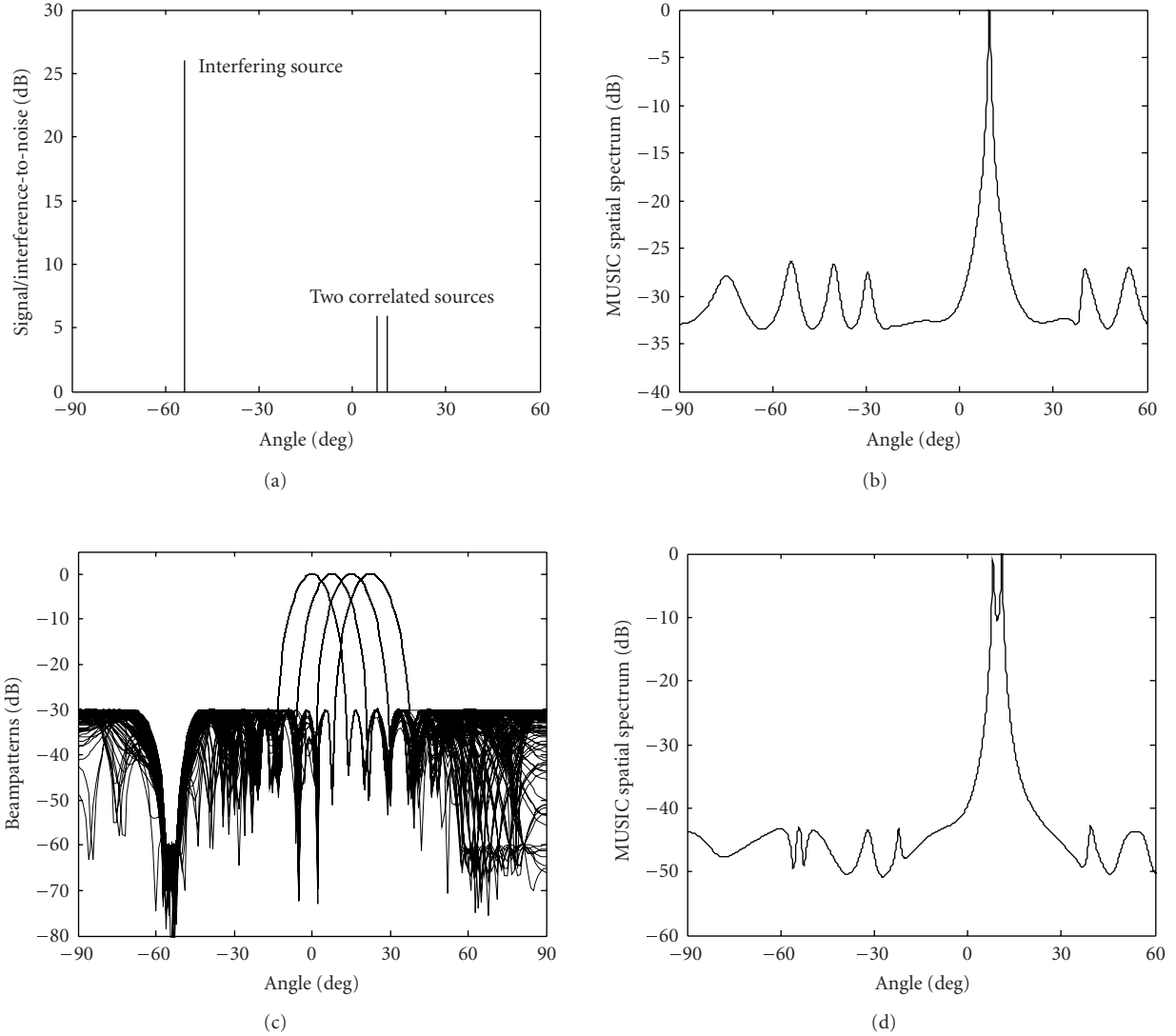


FIGURE 6: DOA estimation for the scenario of strong out-of-sector interfering source. (a) Directions of the two correlated sources and the interfering source. (b) DOA estimation result using the beamformers with uniform sidelobes. (c) Superposition of the notch beampatterns. (d) DOA estimation result using the notch beamformers.

5.2. Interference rejection via notch beamformers

Consider the scenario of strong out-of-sector interfering sources. For the above linear array, the two correlated sources arrived at 8° and 11° with $\text{SNR} = 6$ dB. An interfering source, independent of the wanted sources, arrived at -54° with the interference-to-noise ratio (INR) of 26 dB, as shown in Figure 6(a).

Figure 6(b) shows the spatial spectrum of beamspace MUSIC using the beamformers shown in Figure 3(a). It is seen that the CMRBs with uniformly sidelobe level of -30 dB cannot resolve the correlated sources in the scenario of strong out-of-sector interfering sources.

The $K = 4$ CMRBs that cover the same spatial sector $[0^\circ, 22.5^\circ]$ are designed by setting a notch with the depth of -60 dB and the width of 4° in the direction of the interfering source. The resulting beampatterns are shown in Figure 6(c),

from which it is seen that the mainlobe response is constant over the design band and the prescribed notch is formed on each beampattern. The MUSIC DOA estimation method is used on the K beamformer outputs. The spatial spectrum of the frequency-domain processing approach is shown in Figure 6(d), from which it is seen that our approach is able to resolve correlated source signals in the scenario of strong out-of-sector interfering sources.

6. CONCLUSION

Frequency-domain and time-domain processing approaches to broadband beamspace coherent signal subspace DOA estimation using constant mainlobe response beamforming have been proposed. Our approaches can be applicable to arrays of arbitrary geometry. SOCP-based time-domain and

frequency-domain broadband beamformers with constant mainlobe response are designed. The MUSIC method is then applied to the beamformer outputs to perform the DOA estimation. Computer simulation results show that our frequency-domain and time-domain broadband beamspace DOA estimators exhibit better resolution performance than the existing method. Our DOA estimators maintain good DOA estimation and spatial resolution capability in the scenario of strong out-of-sector interfering sources by setting a notch in the direction of the interfering source.

ACKNOWLEDGMENT

This project was supported by China Postdoctoral Science Foundation.

REFERENCES

- [1] G. Su and M. Morf, "The signal subspace approach for multiple wide-band emitter location," *IEEE Transactions on Acoustics, Speech, and Signal Processing*, vol. 31, no. 6, pp. 1502–1522, 1983.
- [2] M. Wax, T.-J. Shan, and T. Kailath, "Spatio-temporal spectral analysis by eigenstructure methods," *IEEE Transactions on Acoustics, Speech, and Signal Processing*, vol. 32, no. 4, pp. 817–827, 1984.
- [3] H. Wang and M. Kaveh, "Coherent signal-subspace processing for the detection and estimation of angles of arrival of multiple wide-band sources," *IEEE Transactions on Acoustics, Speech, and Signal Processing*, vol. 33, no. 4, pp. 823–831, 1985.
- [4] R. O. Schmidt, "Multiple emitter location and signal parameter estimation," *IEEE Transactions on Antennas and Propagation*, vol. 34, no. 3, pp. 276–280, 1986.
- [5] T.-S. Lee, "Efficient wideband source localization using beamforming invariance technique," *IEEE Transactions on Signal Processing*, vol. 42, no. 6, pp. 1376–1387, 1994.
- [6] D. B. Ward, Z. Ding, and R. A. Kennedy, "Broadband DOA estimation using frequency invariant beamforming," *IEEE Transactions on Signal Processing*, vol. 46, no. 5, pp. 1463–1469, 1998.
- [7] D. B. Ward, R. A. Kennedy, and R. C. Williamson, "FIR filter design for frequency invariant beamformers," *IEEE Signal Processing Letters*, vol. 3, no. 3, pp. 69–71, 1996.
- [8] J. F. Sturm, "Using SeDuMi 1.02, a MATLAB toolbox for optimization over symmetric cones," *Optimization Methods and Software*, vol. 11, no. 1, pp. 625–653, 1999.
- [9] M. S. Lobo, L. Vandenberghe, S. Boyd, and H. Lebert, "Applications of second-order cone programming," *Linear Algebra and Its Applications*, vol. 284, no. 1–3, pp. 193–228, 1998.
- [10] M. Pesavento, A. B. Gershman, and Z.-Q. Luo, "Robust array interpolation using second-order cone programming," *IEEE Signal Processing Letters*, vol. 9, no. 1, pp. 8–11, 2002.
- [11] S. A. Vorobyov, A. B. Gershman, and Z.-Q. Luo, "Robust adaptive beamforming using worst-case performance optimization: a solution to the signal mismatch problem," *IEEE Transactions on Signal Processing*, vol. 51, no. 2, pp. 313–324, 2003.
- [12] S. Yan and Y. L. Ma, "Robust supergain beamforming for circular array via second-order cone programming," *Applied Acoustics*, vol. 66, no. 9, pp. 1018–1032, 2005.
- [13] H. Cox, R. Zeskind, and M. Owen, "Robust adaptive beamforming," *IEEE Transactions on Acoustics, Speech, and Signal Processing*, vol. 35, no. 10, pp. 1365–1376, 1987.
- [14] R. T. Compton Jr., "The relationship between tapped delay-line and FFT processing in adaptive arrays," *IEEE Transactions on Antennas and Propagation*, vol. 36, no. 1, pp. 15–26, 1988.
- [15] L. C. Godara, "Application of the fast Fourier transform to broadband beamforming," *Journal of the Acoustical Society of America*, vol. 98, no. 1, pp. 230–240, 1995.
- [16] H. L. Van Trees, *Detection, Estimation, and Modulation Theory, Part IV, Optimum Array Processing*, John Wiley & Sons, New York, NY, USA, 2002.
- [17] S. Yan, "Optimal design of FIR beamformer with frequency invariant patterns," *Applied Acoustics*, vol. 67, no. 6, pp. 511–528, 2006.
- [18] S. Yan and Y. L. Ma, "A unified framework for designing FIR filters with arbitrary magnitude and phase response," *Digital Signal Processing*, vol. 14, no. 6, pp. 510–522, 2004.
- [19] A. B. Gershman, "Direction finding using beamspace root estimator banks," *IEEE Transactions on Signal Processing*, vol. 46, no. 11, pp. 3131–3135, 1998.

Shenfeng Yan received the B.S., M.S., and Ph.D. degrees in electrical engineering from Northwestern Polytechnical University, Xi'an, China, in 1999, 2001, and 2005, respectively. He is currently a Postdoctoral Fellow with the Institute of Acoustics, Chinese Academy of Sciences, Beijing, China. His current research interests include array signal processing, statistical signal processing, adaptive signal processing, optimization techniques, and signal processing applications to underwater acoustics, radar, and wireless mobile communication systems. He is a member of IEEE.

